Inorganica Chimica Acta, 63 (1982) 197–207

Studies on the Metal–Amide Bond. XVI*. The Coordination Chemistry of the Di-Tertiary Amide Ligand N,N′-Dimethyl-N,N′-bis(2′-pyridinecarboxamide)-1,2-ethane, [bpenMe$_2$], Including the Crystal Structure of *trans*-[Pd(bpenMe$_2$)Cl$_2$]

MOH'D W. MULQI, FREDERICK S. STEPHENS and ROBERT S. VAGG

School of Chemistry, Macquarie University, North Ryde, N.S.W. 2113, Australia

Received April 20, 1982

The isolation and characterization of a number of transition metal complexes of the di-tertiary-amide ligand N,N′-dimethyl-N,N′-bis(2′-pyridinecarboxamide)-1,2-ethane, bpenMe$_2$, is described. Six-coordinate polymeric complexes involving coordination as a [NO]$_2$-bis-bidentate through pyridyl-N and amide-O atoms were obtained with bivalent copper, nickel, cobalt and zinc. N$_2$-Bidentate function through pyridyl-N atoms alone is concluded for complexes of Ag(I), Pt(II) and Pd(II). The crystal structure of [Pd(bpenMe$_2$)Cl$_2$] was determined by X-ray diffraction methods. C$_{16}$H$_{18}$N$_4$O$_2$Cl$_2$Pd is orthorhombic, space group P2$_1$2$_1$2$_1$, with a = *12.229(10),* b = *17.053(13),* c = *8.757(9)* Å *and* Z = *4. The structure was refined to* R *0.072 by least-squares techniques for 1360 photographic reflexions. The coordination geometry about Pd is square planar and the molecule possesses an approximate two-fold rotation axis. The ligand functions as a rare N$_2$-trans-bidentate, coordinating through two pyridyl-N atoms alone [average Pd–N 2.00(1) Å]. The two Cl atoms complete the coordination sphere [average Pd–Cl 2.311(7) Å]. The two picolinamide groups are non-planar, the dihedral angles between the amide group planes and their corresponding pyridine ring planes being 69.7 and 86.1°. The central ethane link has a staggered conformation, the N–C–C–N torsion angle being 58.8°. This rigid structure, with a two-fold rotation axis, is retained in solution. The complex 200 MHz proton n.m.r. spectrum in CDCl$_3$ may be simulated assuming such a structure and H–C–C–H torsion angles calculated from the observed vicinal coupling constants confirm the* gauche *conformation of the central ethane bond in solution. The separate chemical shifts of these methylene protons are explained in terms of the non-planar structure of the ligand in the chelate molecule.*

*Part XV is reference [5].

Introduction

N,N′-Bis(2′-pyridinecarboxamide)-1,2-ethane, bpenH$_2$ *I(a)*, behaves either as a planar N$_4$-tetradentate on deprotonation

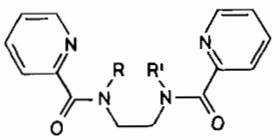

(I)

(a) R = R′ = H; bpenH$_2$
(b) R = H, R′ = CH$_3$ bpenMeH
(c) R = R′ = CH$_3$; bpenMe$_2$

or as a bridging [NO]$_2$-bis-bidentate ligand when in the non-deprotonated form [1–3]. Its monomethyl-N-substituted analogue bpenMeH, *I(b)*, is prevented from acting as an N$_4$-tetradentate by the inability of its constituent tertiary-amide nitrogen atom to coordinate [4, 5]. An interesting divalent palladium deprotonated complex of this ligand, [Pd(bpenMe)Cl], was obtained [4]. Its crystal structure [5] shows the ligand to be acting as an N$_3$-tridentate with the uncoordinated tertiary-amide nitrogen atom incorporated in an unusual eight-membered chelate ring. This same rigid molecular structure is retained on dissolution [5].

As a concurrent and complementary study the coordinating properties of the di-tertiary amide analogue bpenMe$_2$, *I(c)*, have been investigated and details are reported herein. The complex [Pd(bpenMe$_2$)Cl$_2$] was obtained in crystalline form and an account of its X-ray structure analysis is included.

Experimental

Physical measurements and analytical procedures were identical to those outlined previously [1, 5].

0020-1693/82/0000-0000/$02.75

Ligand Synthesis

To a warm solution of 2-pyridinecarboxylic acid (61.5 g, 0.5 mol) in pyridine (200 ml) was added triphenylphosphite (155 g, 0.5 mol) and the mixture was heated for 10 minutes. N,N'-Dimethyl-1,2-diaminoethane (22.0 g, 0.25 mol) in pyridine (50 ml) was then added dropwise with continuous stirring, and the mixture was heated on a steam-bath for 5 h. After volume reduction and cooling chloroform (30 ml) was added and this extract was washed several times with water (20 ml aliquots), with a saturated solution of sodium bicarbonate (20 ml aliquots) and again with water (20 ml aliquots). The chloroform was removed on a steam-bath and, after cooling, absolute ethanol (5–10 ml) was added. Diethylether then was added dropwise with continuous stirring until a permanent precipitate formed. The white solid product was filtered off (40.2 g, 54%). An analytical sample was recrystallized from ethanol to give fine white needles [m.p. 110–112 °C]. *Anal.* Found: C, 64.2; H, 5.8; N, 19.1%. Calcd. for $C_{16}H_{18}N_4O_2$: C, 64.4; H, 6.0; N, 18.8%.

Mass spectrum: m/e (parent) 298.

Preparation of Complexes

Complexes of general formula $Cu(bpenMe_2)X_2 \cdot nH_2O$ (where X = Cl or Br, n = 1; X = NO_3, n = 0.5; and X = ClO_4, n = 0) were prepared by mixing hot equimolar concentrations of the ligand with the appropriate copper(II) salt in aqueous solution. The solid products formed either immediately or after volume reduction on a steam bath. The complexes were filtered off, washed with minimum amounts of water and/or acetone and air-dried.

$Ni(bpenMe_2)(NO_3)_2 \cdot 3H_2O$ and $Ni_2(bpenMe_2)_3(ClO_4)_4 \cdot 3H_2O$ were prepared by mixing a hot aqueous solution of the ligand with hot aqueous solutions of either nickel(II) nitrate or nickel(II) perchlorate hexahydrate in 1:1 mol ratio. The solid products which formed were filtered off, washed with water and ethanol and air-dried.

Complexes of the form $Co(bpenMe_2)X_2 \cdot nH_2O$ (where X = Br, n = 1; X = NO_3, n = 2.5 and X = NCS, n = 0) were prepared by mixing a hot aqueous solution of the ligand with a hot aqueous solution of the appropriate bromide, nitrate, or thiocyanate hydrated salt in 1:1 mol ratio. The products which formed after volume reduction and cooling were filtered off, washed with water and/or acetone and air-dried.

The complexes $Zn(bpenMe_2)I_2 \cdot H_2O$, $Ag(bpenMe_2)ClO_4 \cdot 0.5H_2O$ and $Pt(bpenMe_2)Cl_2 \cdot 3H_2O$ were prepared by a method similar to that described above using ZnI_2, $AgClO_4$ or K_2PtCl_4 as the metal salt.

[Pd(bpenMe$_2$)Cl$_2$]

Attempts to prepare a palladium complex solely from aqueous medium as above resulted in a flocculent solid product which on the basis of thermogravimetric and microanalyses had a composition approximately that of bis(2-picolinato)palladium(II). However, when K_2PdCl_4 in a slight excess was dissolved in a small amount of water and added to a chloroform solution of the ligand and the mixture was covered and allowed to stand overnight with continuous stirring a yellow colour developed in the organic layer. This layer then was separated off and reduced in volume by approximately 80%. After cooling, the slow addition of diethylether caused immediate precipitation of a yellow powder. This product was purified by successive recrystallizations from dimethylformamide/chloroform solvent mixtures (1:5) yielding fine yellow needles.

X-Ray Diffraction Analysis of [Pd(bpenMe$_2$)Cl$_2$]

The complex crystallises as fine yellow needles elongated along [001].

Crystal Data: $[Pd(bpenMe_2)Cl_2]$, $C_{16}H_{18}N_4O_2Cl_2Pd$, M_r = 475.5, Orthorhombic, a = 12.229(10), b = 17.053(13), c = 8.757(9) Å, U = 1826.2 Å^3, D_m = 1.71 (by flotation), Z = 4, D_c = 1.729 Mg m^{-3}, $F(000)$ = 952, $\mu(Cu\text{-}K_\alpha)$ = 11.28 mm^{-1}. Systematic absences: $h0\,0\,8\,0$ if $h \neq 2n$, $0k0$ if $k \neq 2n$ and $00l$ if $l \neq 2n$; space group $P2_12_12_1$ (No. 19).

Cell parameters were determined from oscillation photographs using Cu-K_α radiation. 1679 non-zero reflexions were recorded on layers $h0$–$6l$ and $hk0$–3 from Weissenberg photographs using Cu-K_α radiation. Their intensities were estimated visually and corrected for Lorentz and polarization effects but not for absorption or extinction. The observed structure factors were placed on a common scale by internal correlation. The unique data set thus generated contained 1360 reflexions.

The structure was solved by the heavy-atom method. Refinement was by full-matrix least-squares calculations in which the function minimized was $\Sigma w\Delta^2$. The weight, w, for each reflexion was initially unity, and finally given by $w = (1.0 + 0.10|F_o| + 0.001|F_o|^2)^{-1}$. After isotropic refinement a difference map was calculated which gave approximate positions for all hydrogen atoms. These positions were optimised assuming C–H to be 1.0 Å. They were included in subsequent calculations with a thermal parameter B of 6.0 Å^2 but their parameters were not refined. Refinement was continued with anisotropic thermal parameters for all non-hydrogen atoms, and terminated when the maximum shift in any parameter was $<0.1\,\sigma$. The final value for R, based on 1360 reflexions was 0.072 and for R' $[=(\Sigma w\Delta^2/\Sigma w|F_o|^2)^{1/2}]$ was 0.094. A final difference map showed no unusual features, and a maximum positive electron density of 1.5 eÅ^{-3} associated with the palladium atom.

TABLE I. Analyses of bpenMe$_2$ Complexes (a check on metal analyses is provided in Table VI).

Complex	Found (%)				Required (%)			
	C	H	N	Metal	C	H	N	Metal
Cu(bpenMe$_2$)Cl$_2$·H$_2$O	42.7	4.4	12.6	14.5	42.6	4.4	12.4	14.1
Cu(bpenMe$_2$)Br$_2$·H$_2$O	35.2	3.7	10.5	11.6	35.6	3.7	10.4	11.8
Cu(bpenMe$_2$)(NO$_3$)$_2$·0.5H$_2$O	38.6	3.8	16.9	12.9	38.8	3.8	17.0	12.8
Cu(bpenMe$_2$)(ClO$_4$)$_2$	34.3	3.6	9.7 (Cl: 12.4)	11.5	34.3	3.2	10.0 (Cl: 12.7)	11.3
Ni(bpenMe$_2$)(NO$_3$)$_2$·3H$_2$O	36.6	4.4	16.2	10.8	36.9	4.6	16.1	11.0
Ni$_2$(bpenMe$_2$)$_3$(ClO$_4$)$_4$·3H$_2$O	39.2	4.1	11.4	8.2	39.4	4.1	11.5	8.0
Co(bpenMe$_2$)Br$_2$·H$_2$O	35.9	3.7	10.2	10.9	35.9	3.7	10.5	11.0
Co(bpenMe$_2$)(NO$_3$)$_2$·2.5H$_2$O	36.6	3.8	16.1	11.0	36.5	4.4	16.0	11.2
Co(bpenMe$_2$)(NCS)$_2$	45.6	3.9	17.7 (S: 13.3)	12.6	45.7	3.8	17.6 (S: 13.5)	12.5
Zn(bpenMe$_2$)I$_2$·H$_2$O	29.9	3.1	8.7	10.2	30.2	3.1	8.8	10.3
Ag(bpenMe$_2$)ClO$_4$·0.5H$_2$O	36.7	3.7	11.0		37.1	3.7	10.8	
[Pd(bpenMe$_2$)Cl$_2$]	40.5	3.9	11.6	21.7	40.4	3.8	11.2	22.4
Pt(bpenMe$_2$)Cl$_2$·3H$_2$O	31.0	3.3	8.3	32.3	31.1	3.9	9.1	31.6

TABLE II. Spectral and Magnetic Properties of bpenMe$_2$ Complexes.

Complex	Appearance	Magnetic Moment (B.M.)	λ_{max} (nm)
Cu(bpenMe$_2$)Cl$_2$·H$_2$O	blue	1.86	750
Cu(bpenMe$_2$)Br$_2$·H$_2$O	blue	2.12	660
Cu(bpenMe$_2$)(NO$_3$)$_2$·0.5H$_2$O	blue	1.95	650
Cu(bpenMe$_2$)(ClO$_4$)$_2$	blue	2.10	630
Ni(bpenMe$_2$)(NO$_3$)$_2$·3H$_2$O	pale blue	3.36	895, 640, 540
Ni$_2$(bpenMe$_2$)$_3$(ClO$_4$)$_4$·3H$_2$O	pale blue	3.42	640
Co(bpenMe$_2$)Br$_2$·H$_2$O	yellow	4.95	680
Co(bpenMe$_2$)(NO$_3$)$_2$·2.5H$_2$O	pink	4.60	460(sh)
Co(bpenMe$_2$)(NCS)$_2$	buff	5.10	620, 500(sh)
Zn(bpenMe$_2$)I$_2$·H$_2$O	yellow	diam.	
Ag(bpenMe$_2$)ClO$_4$·0.5H$_2$O	white	diam.	
[Pd(bpenMe$_2$)Cl$_2$]	yellow	diam.	
Pt(bpenMe$_2$)Cl$_2$·3H$_2$O	yellow	diam.	

Results

The analytical data for the complexes isolated are given in Table I. Table II gives their physical appearance and magnetic and spectral properties. Figure 1 shows the reflectance spectra of the paramagnetic complexes in the visible range.

The final atomic coordinates from the X-ray analysis for non-hydrogen atoms, together with estimated standard deviations, are given in Table III. The hydrogen atomic coordinates are given in Table IV and final anisotropic thermal parameters for non-hydrogen atoms in Table V. A list of observed and calculated structure factors has been deposited with the Editor.

The observed magnetic moments of 1.86–2.12 B.M. are quite normal for bivalent copper. The reflectance spectra of the copper complexes show

TABLE III. Final Atomic Coordinates (fractional × 10^4) for Non-Hydrogen Atoms (estimated standard deviations are given in parentheses).

	x	y	z
Pd	886.5(7)	18.9(8)	1191(1)
Cl(1)	−494(4)	−73(3)	3008(6)
Cl(2)	2403(3)	127(3)	−342(5)
N(11)	857(14)	1191(8)	1318(18)
N(21)	995(11)	−1141(8)	1001(16)
N(1)	−758(13)	903(10)	−1414(21)
N(2)	−403(12)	−761(10)	−2055(20)
O(1)	779(10)	1476(10)	−2418(15)
O(2)	−1500(10)	−1195(8)	−94(20)
C(1)	−1035(18)	576(16)	−2880(27)
C(2)	−1321(16)	−330(13)	−2702(28)
C(N1)	−1556(16)	875(15)	−231(35)
C(N2)	649(18)	−781(16)	−2930(27)
C(11)	526(16)	1656(11)	215(30)
C(12)	602(18)	2502(12)	349(27)
C(13)	1004(18)	2806(12)	1570(36)
C(14)	1402(17)	2308(15)	2754(42)
C(15)	1287(19)	1532(11)	2568(27)
C(21)	358(13)	−1584(11)	−17(22)
C(22)	481(16)	−2373(10)	−179(29)
C(23)	1261(16)	−2737(11)	709(28)
C(24)	1920(15)	−2339(13)	1672(28)
C(25)	1757(15)	−1538(11)	1814(27)
C(01)	198(14)	1334(11)	−1286(24)
C(02)	−565(15)	−1133(11)	−752(24)

TABLE IV. Hydrogen Atomic Coordinates (fractional × 10^3).

	x	y	z
H(12)	35	285	−50
H(13)	104	339	169
H(14)	175	253	369
H(15)	154	118	342
H(22)	2	268	−91
H(23)	134	−332	64
H(24)	251	−261	226
H(25)	222	−124	255
H(1a)	−168	86	−331
H(1b)	−40	64	−359
H(2a)	−150	−55	−373
H(2b)	−197	−39	−201
H(CN1a)	−142	132	−52
H(CN1b)	−230	94	−68
H(CN1c)	−151	36	31
H(CN2a)	−108	−30	−257
H(CN2b)	50	−75	−405
H(CN2c)	106	−127	−270

broad d–d transition maxima in the range 630–750 nm. As is shown in Fig. 1 these maxima shift to higher frequencies in the order $Cl^- < Br^- < NO_3^- < ClO_4^-$ suggesting coordination of the halide anions in the solid state. The nickel and cobalt complexes have magnetic moments and spectra typical of high-spin octahedral forms for those metals.

Table VI gives the results of thermogravimetric studies performed on the complexes. Similar to the metal complexes of related ligands [2, 4] the halide complexes of cobalt, zinc and copper, with the exception of the latter chloride, show weight loss patterns attributable to partial sublimation.

The characteristic infrared bands of the ligand and its metal complexes are given in Table VII. The free ligand shows a strong band at 1636 cm^{-1} assigned to the Amide I absorption. For all the first-row transition metal complexes this band shifts to lower frequencies, indicating coordination of the amide groups. This is confirmed by a significant shift in the amide out-of-plane deformation band at 650 cm^{-1} to higher frequencies on coordination. The pyridine ring deformation band at 618 cm^{-1} shifts to higher frequencies in all complexes, indicating also pyridyl-N coordination. In addition the spectrum of the palladium complex shows a strong

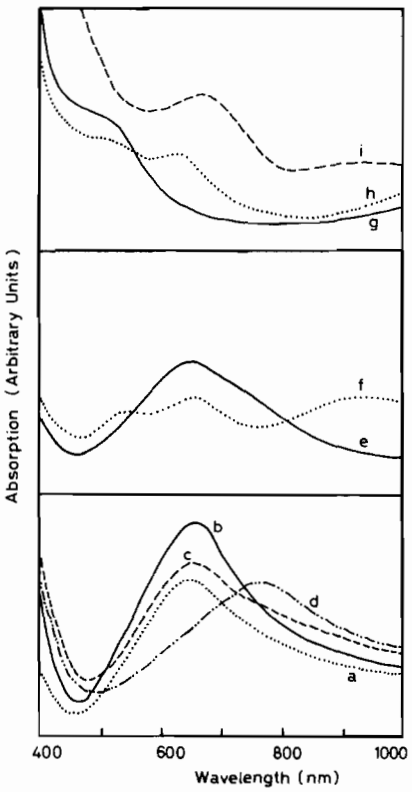

Fig. 1. Diffuse reflectance spectra of $bpenMe_2$ complexes. (a) $Cu(bpenMe_2)(ClO_4)_2$; (b) $Cu(bpenMe_2)(NO_3)_2 \cdot 0.5H_2O$; (c) $Cu(bpenMe_2)Br_2 \cdot H_2O$; (d) $Cu(bpenMe_2)Cl_2 \cdot H_2O$; (e) $Ni_2(bpenMe_2)_3(ClO_4)_4 \cdot 3H_2O$; (f) $Ni(bpenMe_2)(NO_3)_2 \cdot 3H_2O$; (g) $Co(bpenMe_2)(NO_3)_2 \cdot 2.5H_2O$; (h) $Co(bpenMe_2)(NCS)_2$; (i) $Co(bpenMe_2)Br_2 \cdot H_2O$.

TABLE V. Final Anisotropic Thermal Parameters ($\times 10^4$) [in the form exp $-(h^2b_{11} + k^2b_{22} + l^2b_{33} + 2hkb_{12} + 2hlb_{13} + 2klb_{23})$, with estimated standard deviations in parentheses].

	b_{11}	b_{22}	b_{33}	b_{12}	b_{13}	b_{23}
Pd	40.1(6)	22.1(4)	92.2(2)	4(5)	−75(7)	−1(2)
Cl(1)	67(3)	34(2)	135(6)	5(2)	20(4)	1(6)
Cl(2)	56(2)	38(2)	120(5)	−2(2)	7(3)	−6(5)
O(1)	47(8)	61(8)	115(19)	6(7)	8(11)	20(13)
O(2)	54(8)	41(5)	138(24)	−3(6)	31(13)	22(13)
N(11)	81(12)	22(4)	47(18)	13(7)	8(15)	−5(12)
N(21)	53(9)	24(4)	38(17)	12(6)	−10(11)	22(11)
N(1)	54(10)	46(7)	106(22)	7(8)	−11(16)	21(16)
N(2)	58(10)	38(6)	95(22)	−2(7)	17(14)	31(15)
C(1)	74(16)	70(13)	94(28)	−18(12)	−56(19)	11(21)
C(2)	54(12)	50(8)	123(30)	−1(9)	−32(17)	−3(20)
C(N1)	47(12)	60(10)	202(44)	3(10)	−16(22)	−23(28)
C(N2)	47(11)	67(11)	109(27)	−15(10)	11(16)	26(21)
C(11)	51(12)	26(6)	152(36)	2(7)	−13(18)	4(20)
C(12)	82(18)	29(6)	132(35)	5(10)	68(22)	−3(20)
C(13)	78(16)	30(7)	241(48)	−3(9)	86(25)	−49(22)
C(14)	59(15)	50(10)	351(70)	4(11)	56(29)	−62(31)
C(15)	96(16)	20(6)	139(3)	−9(9)	−3(21)	12(18)
C(21)	39(10)	39(7)	57(22)	−11(7)	9(13)	2(17)
C(22)	63(14)	29(7)	134(35)	−1(8)	−12(19)	−8(19)
C(23)	64(13)	29(6)	177(37)	−2(8)	33(21)	−41(20)
C(24)	58(13)	43(8)	152(35)	5(9)	−19(18)	0(23)
C(25)	63(12)	29(6)	147(33)	−3(8)	−46(18)	−13(21)
C(01)	47(11)	35(7)	117(29)	1(7)	−13(15)	6(17)
C(02)	58(13)	32(6)	126(31)	−3(8)	−46(17)	−14(17)

For all hydrogen atoms $B = 6.0$ Å^2.

TABLE VI. Results of Thermogravimetric Studies on $bpenMe_2$ Complexes.

Complex	Temp. Range (°C)	Vol. Products[a]	Wt. Loss (%)		Metal	
			Found[b]	Calc.	Found[c]	Calc.
$Cu(bpenMe_2)Cl_2 \cdot H_2O$	35–280	H_2O	3.0	4.0		
	410–670	$bpenMe_2$	82.6	81.9		
		Total Loss	85.6	85.9	14.4	14.1
$Cu(bpenMe_2)Br_2 \cdot H_2O$[d]	65–225	H_2O	3.2	3.3	–	–
$Cu(bpenMe_2)(NO_3)_2 \cdot 0.5H_2O$[e]	80–190	$0.5H_2O$	1.5	1.8	–	–
$Ni(bpenMe_2)(NO_3)_2 \cdot 3H_2O$[e]	50–145	$3H_2O$	9.5	10.1	–	–
$Ni_2(bpenMe_2)_3(ClO_4)_4 \cdot 3H_2O$[e]	35–170	$3H_2O$	3.7	3.7	–	–
$Co(bpenMe_2)Br_2 \cdot H_2O$[d]	80–180	H_2O	3.0	3.3	–	–
$Co(bpenMe_2)(NO_3)_2 \cdot 2.5H_2O$[e]	80–190	$2H_2O$	6.0	6.1	–	–
$Co(bpenMe_2)(NCS)_2$	290–440	$bpenMe_2$	62.0	63.0		
	460–645	$2SO_2$	15.0	13.7		
		Total Loss	77.0	76.7	12.2	12.5
$Zn(bpenMe_2)I_2 \cdot H_2O$[d]	95–280	H_2O	3.0	2.8	–	–
$Ag(bpenMe_2)ClO_4 \cdot 0.5H_2O$[e]	18–180	$0.5H_2O$	1.0	1.7	–	–
$Pd(bpenMe_2)Cl_2$	260–550	$bpenMe_2$ + Cl_2	78.3	77.6	21.7	22.4

(continued overleaf)

TABLE VI. *(continued)*

Complex	Temp. Range (°C)	Vol. Products[a]	Wt. Loss (%)		Metal	
			Found[b]	Calc.	Found[c]	Calc.
$Pt(bpenMe_2)Cl_2 \cdot 3H_2O$	35–260	$3H_2O$	9.0	8.7		
	290–680	$bpenMe_2$				
		$+Cl_2$	58.7	59.7		
		Total Loss	67.7	68.4	32.3	31.6

[a]$bpenMe_2$ = N,N'-dimethyl,N,N'-bis(2'-pyridinecarboxamide)-1,2-ethane. [b]Final weight loss corrected for uptake of oxygen. [c]Assuming CuO, $Co(CN)_2$, Pd and Pt to be the residues for the respective metals. [d]Decomposition patterns and residue weights for these complexes were not found to be reproducible, possibly due to partial sublimation. [e]Nitrate and perchlorate complexes were studied below 200 °C to prevent possible explosion.

TABLE VII. Characteristic Infrared Bands with Tentative Assignments.[a]

Compound	ν(O–H)	Amide I[b]	ν(C–N)[b]	δ(NCO)[b]	Py. Ring[d]	Other Bands
$bpenMe_2$		1636(ss)	1405(ms)	652(s)	618(2)	
$Cu(bpenMe_2)Cl_2 \cdot H_2O$	3400(br)	1632(s)	1430(s)	700(s)	650(s)	
$Cu(bpenMe_2)Br_2 \cdot H_2O$	3400(br)	1605(ms)	1435(s)	685(s)	660(w)	
$Cu(bpenMe_2)(NO_3)_2 \cdot 0.5H_2O$	3400(br)	1605(ms)	1425(ms)	685(s)	660(w)	1380(br) ν(N–O)
$Cu(bpenMe_2)(ClO_4)_2$	–	1610(ms)	1422(s)	685(ss)	660(w)	1100(sbr)[e]
$Ni(bpenMe_2)(NO_3)_2 \cdot 3H_2O$	3250(br)	1610(s)	[f]	690(s)	650(w) 660(ms)	1380(br) ν(N–O)
$Ni_2(bpenMe_2)_3(ClO_4)_4 \cdot 3H_2O$	3300(br)	1610(s)	1420(ms)	700(s)	660(s)	1100(sbr)[e]
$Co(bpenMe_2)Br_2 \cdot H_2O$	3400(br)	1615(ss)	1430(s)	700(ss)	640(s) 660(ss)	
$Co(bpenMe_2)(NO_3)_2 \cdot 2.5H_2O$	3300(br)	1610(s)	[f]	695(s) 675(ms)	642(w)	1380(br) ν(N–O)
$Co(bpenMe_2)(NCS)_2$	–	1608(s)	1425(w)	700(ss)	640(s) 660(s)	2090(ss) ν(C≡N)
$Zn(bpenMe_2)I_2 \cdot H_2O$	3450(br)	1610(ms)	1425(ms)	690(ms) 680(ms)	658(s)	
$Ag(bpenMe_2)ClO_4 \cdot 0.5H_2O$	3450(br)	1640(ss)	1405(ms)	650(s)	630(ss)	1090(sbr)[e]
$[Pd(bpenMe_2)Cl_2]$		1635(ss)	1405(ms)	650(ms)	[g]	
$Pt(bpenMe_2)Cl_2 \cdot 3H_2O$	3500(br)	1640(ss)	1408(ms)	650(w)	[g]	

[a]ss = strong and sharp; s = strong; ms = medium strong; br = broad; sbr = strong and broad; w = weak. [b]From reference [6]. [c]From reference [15]. [d]Pyridine ring in-plane deformation [7, 16]. [e]Ionic perchlorate absorption. [f]Obscured by ν(N–O). [g]Obscured by δ(NCO).

band at 345 cm^{-1} which is in the region diagnostic of ν(Pd–Cl) with a *trans* arrangement [6, 7].

Details of the proton n.m.r. spectra of $bpenMe_2$ and its palladium complex are given in Table VIII. The multiplicity of the signals for the protons of the free ligand, and the methyl and methylene protons in particular, may be interpreted as arising from an unequal population of isomers derived from combinations of *cis*- and *trans*-amide forms [5]. In $[Pd(bpenMe_2)Cl_2]$, however, the six methyl hydrogen atoms are magnetically equivalent, evidenced by a sharp singlet at δ 3.18. The methylene proton signals due to H(1b) and H(2b) show a large shift (334 Hz) to lower field strengths in this complex, whereas those of H(1a) and H(2a) are shifted 144 Hz to higher fields. This is in marked contrast with the methylene proton signals of the planar tetradentate chelates Pd(bpen) [2] and Pd(6-mebpen) [8],

TABLE VIII. Results of Proton NMR Studies in $CDCl_3$.

(a) Chemical shift (ppm)[a]:

	$bpenMe_2$	$[Pd(bpenMe_2)Cl_2]$
H(12), H(22)	7.72(m)	7.88(d)
H(13), H(23)	7.60(m)	7.50(m)
H(14), H(24)	7.32(m)	7.42(m)
H(15), H(25)	8.52(m)	8.91(d)
H(1a), H(2a)	3.75(m), 3.82(s)	3.10(q)
H(1b), H(2b)	3.88(s)	5.49(q)
CH_3	2.91(s), 3.01(s), 3.18(s), 3.25(s)	3.18(s)

(b) Coupling constants (Hz) of methylene protons obtained from the spectrum of $[Pd(bpenMe_2)Cl_2]$.

$J_{(1a,1b)} = J_{(2a,2b)} = (-)13.28$ $J_{(1a,2a)} = 1.00$

$J_{(1a,2b)} = J_{(1b,2a)} = 2.62$ $J_{(1b,2b)} = 10.00$

[a]m = multiplet; q = quartet; d = doublet; s = singlet.

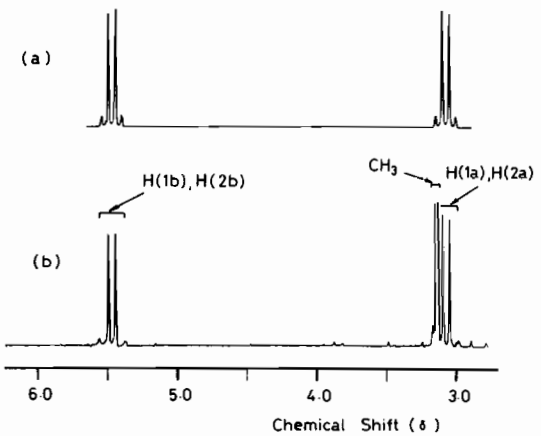

Fig. 2. Computer simulation of signals for methylene protons in $[Pd(bpenMe_2)Cl_2]$. (a) Simulated spectrum using coupling constants and chemical shifts given in Table VIII. (b) Observed spectrum.

which are little removed from those of their respective free ligands. Figure 2 shows a computer simulated spectrum [9] of these methylene protons using coupling constants as given in Table VIII, together with the observed spectrum in the range δ 3.0–6.0.

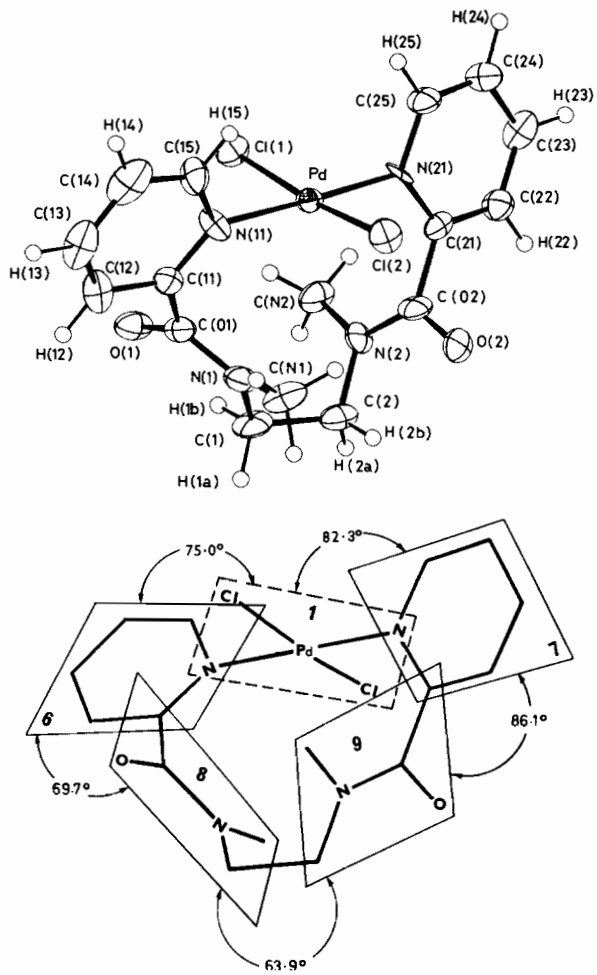

Fig. 3. A perspective drawing [17] of the molecule showing the atomic labelling scheme, and a trigonometric projection illustrating the primary planes of the molecule numbered according to Table XI. Thermal ellipsoids are scaled to include 35% probability. Hydrogen atoms have been included with a thermal parameter of $B = 1.0$ Å^2.

Description of the Crystal Structure of $[Pd(bpenMe_2)Cl_2]$

Bond lengths and angles in the molecule are given in Table IX. Figure 3 shows a perspective drawing of the molecule with atom labelling. The molecular packing in the unit cell is shown in Figure 4. All intermolecular contacts less than 3.5 Å are listed in Table X. The closest non-bonded intermolecular contact is 3.09(2) Å between O(1) and C(25) at $\frac{1}{2} - x, \bar{y}, z - \frac{1}{2}$. Least-squares planes for the pyridine rings, the two amide groups and the N_2Cl_2 coordination plane are listed in Table XI and illustrated in a trigonometric projection of the molecule in Fig. 3.

The molecule possesses an approximate two-fold rotation axis in the solid state passing through the palladium atom and the centre of the C(1)–C(2)

TABLE IX. Bond Lengths (Å) and Angles (°) with Estimated Standard Deviations in Parentheses.

	n = 1	n = 2
Pd–Cl(n)	2.325(4)	2.297(4)
Pd–N(n1)	2.00(1)	1.99(1)
N(n1)–C(n1)	1.32(3)	1.41(2)
N(n1)–C(n5)	1.35(3)	1.35(2)
N(n)–C(0n)	1.39(2)	1.32(2)
N(n)–C(n)	1.44(3)	1.46(2)
N(n)–C(Nn)	1.42(3)	1.50(2)
C(n1)–C(n2)	1.45(3)	1.36(3)
C(n1)–C(0n)	1.48(3)	1.51(3)
C(n2)–C(n3)	1.29(4)	1.38(3)
C(n3)–C(n4)	1.43(4)	1.35(3)
C(n4)–C(n5)	1.34(3)	1.39(3)
C(0n)–O(n)	1.24(2)	1.29(2)
C(1)–C(2)	1.59(3)	
Cl(1)–Pd–Cl(2)	172.6(2)	Cl(1)–Pd–N(21) 92.2(4)
Cl(2)–Pd–N(11)	88.1(5)	N(11)–Pd–N(21) 176.8(6)
N(1)–C(1)–C(2)	110(2)	N(2)–C(2)–C(1) 111(2)
N(n1)–Pd–Cl(n)	90.9(5)	88.7(4)
Pd–N(n1)–C(n1)	125(1)	124(1)
Pd–N(n1)–C(n5)	118(1)	120(1)
C(n1)–N(n1)–C(n5)	117(2)	117(1)
C(n)–N(n)–C(On)	119(2)	118(2)
C(n)–N(n)–C(Nn)	118(2)	118(2)
C(On)–N(n)–C(Nn)	123(2)	124(2)
N(n1)–C(n1)–C(n2)	121(2)	123(2)
N(n1)–C(n1)–C(On)	121(2)	114(2)
C(n2)–C(n1)–C(On)	117(2)	123(2)
C(n1)–C(n2)–C(n3)	120(2)	118(2)
C(n2)–C(n3)–C(n4)	120(2)	123(2)
C(n3)–C(n4)–C(n5)	118(3)	118(2)
C(n4)–C(n5)–N(n1)	125(3)	123(2)
N(n)–C(On)–C(n1)	120(3)	120(2)
N(n)–C(On)–O(n)	121(2)	124(2)
C(n1)–C(On)–O(n)	119(2)	116(2)

TABLE X. Intermolecular Distances < 3.5 Å.[a]

Cl(2) . . . . . .C($N2^{I}$)	3.37(2)
C(14) . . . . . .O(2^{II})	3.28(2)
C(14) . . . . . .C(21^{II})	3.48(3)
C(14) . . . . . .C(22^{II})	3.18(3)
O(1) . . . . . .C(22^{III})	3.26(3)
O(1) . . . . . .C(24^{IV})	3.27(3)
O(1) . . . . . .C(25^{IV})	3.09(2)
O(2) . . . . . .C(23^{V})	3.33(2)
O(2) . . . . . .C(24^{V})	3.45(2)

[a]Roman numeral superscripts refer to the following equivalent positions relative to x, y, z:
I $\frac{1}{2} - x, \bar{y}, \frac{1}{2} + z$
II $\bar{x}, \frac{1}{2} + y, \frac{1}{2} - z$
III $\bar{x}, \frac{1}{2} + y, \bar{z} - \frac{1}{2}$
IV $\frac{1}{2} - x, \bar{y}, z - \frac{1}{2}$
V $x - \frac{1}{2}, \bar{y} - \frac{1}{2}, \bar{z}$

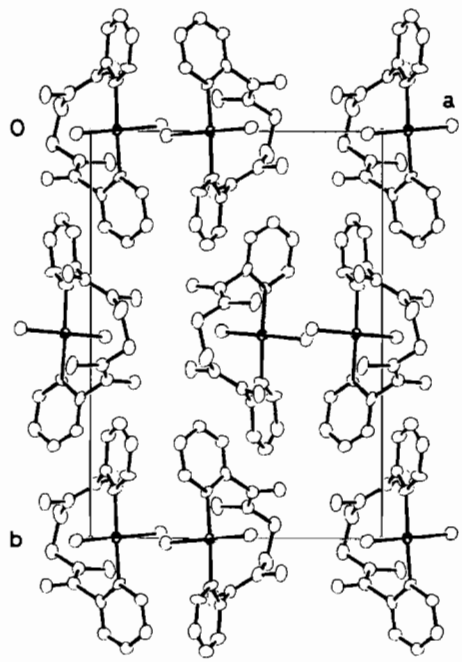

Fig. 4. Molecular packing in the cell viewed down *c*.

bond. The ligand has the rare function of acting as a *trans*-bidentate, coordinating to the metal atom through the two pyridyl nitrogen atoms alone. This generates a highly unusual eleven-membered chelate ring. The two chlorine atoms complete a distorted square-planar coordination (Table XI, plane 1). The coordination plane shows a 6.0° tetrahedral twist (Table XI, planes 2–5) at the palladium atom. The average Pd–N(*pyridine*) and Pd–Cl bond distances are 2.00(1) and 2.311(7) Å respectively, which are similar to those found in [Pd(bpenMe)Cl] [5].

The two pyridine rings are planar within experimental error (Table XI, planes 6 and 7) and their planes are rotated by 75.0 and 82.3° respectively relative to the N_2Cl_2 plane (Fig. 3), with the palladium atom being slightly displaced from each pyridine plane. Each of the two amide groups is nearly planar (Table XI, planes 8 and 9) and has a *trans*-arrangement. The dihedral angles between each amide group plane and its corresponding pyridine ring plane are 69.7 and 86.1° respectively and hence there is little likelihood of any π-conjugation in the picolinamide groups. The Pd···C(01) and Pd···C(02) dis-

TABLE XI. Least-squares Planes Data.

(a) Least-squares planes and their equations given by $lX + mY + nZ - p = 0$. Deviations (Å) of relevant atoms from the planes are given in square brackets.

	l	*m*	*n*	*p*
Plane (1): N(11), Cl(1), N(21), Cl(2)	0.6397	−0.0268	0.7682	1.5727
[N(11) −0.070; Cl(1) 0.067; N(21) −0.069; Cl(2) 0.072; Pd −0.08]				
Plane (2): Cl(1), N(11), Cl(2)	0.6346	0.0431	0.7716	1.6435
[Pd −0.15]				
Plane (3): Cl(1), N(21), Cl(2)	0.6402	−0.0954	0.7622	1.6327
[Pd −0.15]				
Plane (4): N(11), Cl(1), N(21)	0.6828	−0.0221	0.7303	1.5138
[Pd −0.01]				
Plane (5): N(11), Cl(2), N(21)	0.5902	−0.0314	0.8067	1.4861
[Pd −0.01]				
Plane (6): N(11), C(11)–(15)	0.9073	−0.0283	−0.4195	0.4163
[N(11) −0.007; C(11) 0.009; C(12) 0.003; C(13) −0.015; C(14) 0.016; C(15) −0.006; Pd 0.13; C(01) 0.21]				
Plane (7): N(21), C(21)–(25)	−0.6694	−0.1517	0.7273	0.1118
[N(21) 0.007; C(21), C(22) −0.006; C(23) 0.016; C(24) −0.014; C(25) 0.003; Pd −0.08; C(02) 0.16]				
Plane (8): C(11), C(01), O(1), N(1), C(1), C(N1)	−0.4706	0.8468	−0.2481	2.1086
[C(11) −0.066; C(01) −0.017; O(1) 0.100; N(1) −0.062; C(1) −0.056; C(N1) 0.101; Pd −2.85]				
Plane (9): C(21), C(02), O(2), N(2), C(2), C(N2)	−0.2669	−0.8175	−0.5103	2.1318
[C(21) −0.032; C(02) −0.033, O(2) 0.065; N(2) −0.021; C(2) −0.034; C(N2) 0.055; Pd −2.98]				
Plane (10): C(1), N(1), C(2), N(2)	0.7838	0.1359	−0.6059	0.3803
[N(1) −0.147; C(1) 0.289; C(2) −0.289; N(2) 0.147]				
Plane (11): N(1), C(1), C(2)	−0.9605	0.2328	0.1527	1.0594
Plane (12): N(2), C(1), C(2)	0.3512	−0.1727	−0.9202	1.7069

(b) Dihedral angles (°) between selected planes.

1–6	75.0	2–3	8.0	6–8	69.7
1–7	82.3	2–4	5.2	7–9	86.1
		2–5	5.4	8–9	63.9
		3–4	5.2	11–12	58.8
		3–5	5.3		
		4–5	6.9		

tances of 3.23(2) and 3.15(2) Å respectively represent the closest non-bonding intramolecular contacts between the metal atom and the amide group.

The methylene hydrogen atoms of the central link adopt a *gauche* conformation, the N(1)–C(1)–C(2)–N(2) torsion angle being 58.8° (Table XI, planes 11 and 12).

Discussion

This study again shows the tertiary-amide nitrogen atom to remain unreactive towards metal coordination, at least when incorporated as part of a linear multidentate. The complexes isolated of bpenMe$_2$ with the first-row transition metals are very similar to the non-deprotonated complexes of bpenH$_2$ [2]

and bpenMeH [4] with those metals. Bis-bidentate $[NO]_2$ coordination is indicated in each case, with amide-O coordination being evidenced in particular by a 20–40 cm^{-1} decrease in the frequency of the Amide I band in the infrared spectra. These similarities extend also to the magnetic, thermal and visible–spectral properties of the complexes, and indeed may be taken as confirming the mode of bonding in the unsubstituted ligands. The polymeric structures proposed earlier [2, 4] are obvious for these 1:1 complexes, with halide ions included in the coordination spheres. It is of interest that a nickel perchlorate complex of 2:3 stoichiometry now has been isolated with each flexible ligand tested, including those with a central link of 1,2-cyclohexane [10] and 1,3-propane [11]. The dimeric N_3O_3 coordination geometry proposed for these salts [2] may be the result of crystal lattice stabilization of the $[Ni_2(ligand)_3]^{4+}$ by the larger anion, although it must also reflect the non-coordinating behaviour of the perchlorate group.

Such geometries do not appear to be so for the complexes of silver, platinum and palladium. In each of these complexes pyridyl-N coordination only is indicated from the infrared data, and the mode of this coordination is demonstrated in the crystal structure of the Pd compound.

The effect of progressive substitution of the amide-N atoms is best demonstrated by the series of Pd complexes shown in *II(a)–(c)*.

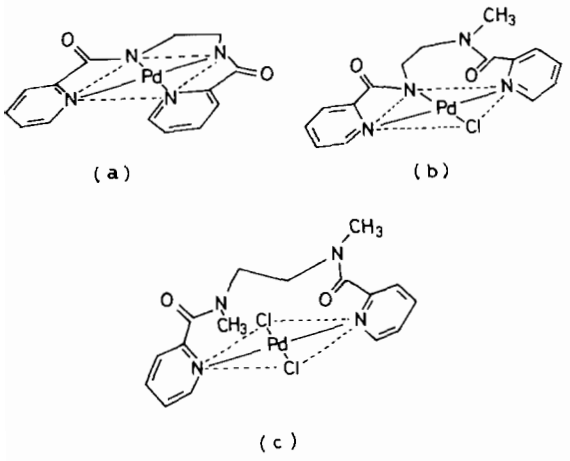

(a) $[Pd(bpen)]\,2H_2O$
(b) [Pd(bpenMe)Cl]
(c) $[Pd(bpenMe_2)Cl_2]$ (II)

The planar N_4-tetradentate behaviour of the unsubsituted ligand $bpenH_2$ on deprotonation, as shown in *II(a)*, has been demonstrated in the crystal structure of the nickel chelate [3]. The mono-N-methylated ligand bpenMeH acts as an N_3-tridentate in forming the complex shown in *II(b)*, and an unusual eight-membered chelate ring results [5]. With both amide N atoms methylated the ligand $bpenMe_2$ acts as an unusual *trans* N_2-bidentate alone in the complex shown in *II(c)* (and Fig. 3). The steric hindrance effects present in $[Pd(bpen)]\cdot 2H_2O$ due to interaction of the 6-pyridyl hydrogen atoms [2] would be relieved in the N-substituted chelates by the pyridyl groups not being coordinated in adjacent sites on the metal atom. The *trans* bidentate arrangement observed in $[Pd(bpenMe_2)Cl_2]$ had been suggested earlier as a means of relieving strain in a closely related sterically hindered chelate [8], and a similar coordination mode was proposed for silver(I) and platinum(II) complexes of $bpbH_2$ [12], $bpenH_2$ [2] and $bpchH_2$ [10]. A few other examples of *trans* bidentate function have been verified, and the subject has been reviewed recently [13].

Unfortunately the insoluble nature of the platinum and silver complexes of $bpenMe_2$ prevented comparison with the n.m.r. spectrum of the palladium complex as given in Table VIII. That the two methyl groups in the chelate have the same chemical shift, and so also the two vicinal proton pairs of the ethane link, is in accord with the molecule possessing a two-fold axis of symmetry in solution.

The large down-field shift of the two protons H(1b) and H(2b) reflects the deshielding effect of the two nearby carbonyl groups, demonstrated in the crystal structure by the interatomic distances O(1)····H(1b) = 2.28 Å and O(2)····H(2b) = 2.25 Å. These distances are almost identical to the carboxyl contact distance observed for the de-shielded proton in the structure of [Pd(bpenMe)Cl] [5]. The high-field resonance positions for H(1a) and H(2a) would most likely result from the non-planar nature of the ligand in the chelate molecule, resulting in a loss of deshielding by the pyridine groups.

Use of the Karplus equation [14] to calculate torsion angles derived from the observed coupling constants (Table VIII(b)) confirms that the molecular structure observed in the solid state is retained in solution. The staggered conformation of the central ethane link is shown in projection in Fig. 5, where these calculated H–C–C–H torsion angles may be compared with that of 58.8° observed in the solid state for N(1)–C(1)–C(2)–N(2). The H(1b)H(2b) coupling constant of 10.0 Hz is consistent with those hydrogen atoms adopting an *anti* configuration [14], whereas H(1a) and H(2a) have a *gauche* relationship with other vicinal protons. The correlation of X-ray and n.m.r data demonstrates the rigid nature of the chelate.

Again a similar inflexibility was demonstrated in the structure of the mono-substituted analogue [5]. In that case a closely eclipsed conformation of the central link is observed. Both complexes demonstrate vividly the inability of the ligands'

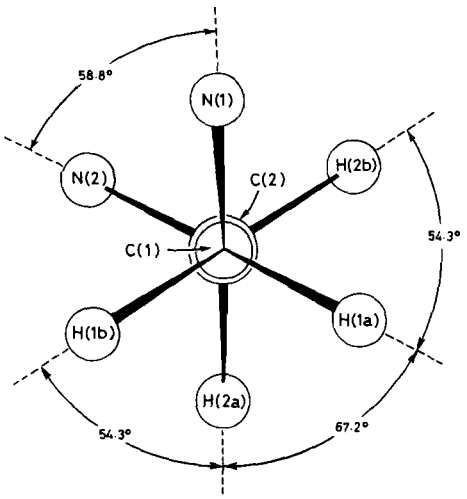

Fig. 5. Projection down the C(1)–C(2) bond showing H–C–C–H torsion angles calculated from vicinal coupling constants given in Table VIII. The N–C–C–N torsion angle derived from the crystal structure analysis also is shown.

constituent tertiary-amide nitrogen atoms to coordinate. They demonstrate also the analytical value of infrared and high resolution n.m.r. spectroscopy when applied to such compounds.

Acknowledgements

The authors thank Dr. M. Batley and Mr. A. Tseng for assistance with the recording and simulation of p.m.r. spectra. One of us (M. M.) wishes to thank the Australian Development Assistance Bureau for a post-graduate research award.

References

1 R. L. Chapman, F. S. Stephens and R. S. Vagg, *Acta Cryst., B37,* 75 (1981).
2 D. J. Barnes, R. L. Chapman, F. S. Stephens and R. S. Vagg, *Inorg. Chim. Acta, 51,* 155 (1981).
3 F. S. Stephens and R. S. Vagg, *Inorg. Chim. Acta, 57,* 9 (1982).
4 M. Mulqi, F. S. Stephens and R. S. Vagg, *Inorg. Chim. Acta, 62,* 215 (1982).
5 M. Mulqi, F. S. Stephens and R. S. Vagg, *Inorg. Chim. Acta, 62,* 221 (1982).
6 L. J. Bellamy, 'The Infrared Spectra of Complex Molecules', Chapman and Hall, 3rd Edition, London (1975).
7 R. J. H. Clark and C. S. Williams, *Inorg. Chim. Acta, 4,* 350 (1965).
8 R. L. Chapman, F. S. Stephens and R. S. Vagg, *Inorg. Chim. Acta, 52,* 161 (1981).
9 A. A. Bothner-By and S. M. Castellano, *J. Chem. Phys., 41,* 3863 (1964).
10 M. Mulqi, F. S. Stephens and R. S. Vagg, *Inorg. Chim. Acta, 53,* L91 (1981).
11 W. H. Saxby, F. S. Stephens and R. S. Vagg, unpublished results.
12 R. L. Chapman and R. S. Vagg, *Inorg. Chim. Acta, 33,* 227 (1979).
13 J. C. Bailar, Jr., *J. Chem. Ed., 58,* 674 (1981).
14 K. A. McLauchlan, 'Magnetic Resonance', Clarendon Press, Oxford, p. 68 (1972).
15 H. O. Desseyn, B. J. Van der Veken and M. A. Herman, *Spectrochim. Acta, 33A,* 633 (1977).
16 M. Nonoyama and K. Yamasaki, *Inorg. Chim. Acta, 3,* 585 (1969).
17 C. K. Johnson, ORTEP (1965). Report ORNL-3794, revised 1971. Oak Ridge National Laboratory, Tennessee.